PAPERS | AUGUST 01 2024

Four interacting spins: Addition of angular momenta, spin–spin correlation functions, and entanglement

Raimundo R. dos Santos; Lucas Alves Oliveira; Natanael C. Costa

Am. J. Phys. 92, 606–615 (2024)
https://doi.org/10.1119/5.0150433

Four interacting spins: Addition of angular momenta, spin–spin correlation functions, and entanglement

Raimundo R. dos Santos,[a] Lucas Alves Oliveira,[b] and Natanael C. Costa[c]
Instituto de Física, Universidade Federal do Rio de Janeiro, 21941-972 Rio de Janeiro, RJ, Brazil

(Received 14 March 2023; accepted 13 May 2024)

We study four spins on a ring coupled through competing Heisenberg interactions between nearest neighbors, J, and next-nearest neighbors, $J_2 \equiv \alpha J > 0$. From the pedagogical point of view, dealing with few spins illustrates how to add more than two angular momenta in a systematic way. The spectrum is obtained by using the rules for addition of four angular momenta, which allows us to follow the evolution of the ground state with α, characterized by level crossings and by spin–spin correlation functions. The reduced number of spins also allows us to illustrate how to quantify bipartite entanglement.

https://doi.org/10.1119/5.0150433

I. INTRODUCTION

Some many-body systems are characterized by the presence of a quantum critical point occurring at zero absolute temperature, which generically separates an ordered (or quasi-ordered) phase from a disordered one. This phase transition is driven by some control parameter,[1,2] which, for magnetic systems, may be an external transverse field, competing interactions, the doping fraction or pressure. Despite being a zero temperature (that is, ground state) phenomenon, the presence of a quantum critical point influences the behavior of measurable quantities at finite temperatures.[1,2] Given that the singularities appearing in second-order phase transitions only manifest themselves in the thermodynamic limit, a widely used theoretical strategy to study measurable properties is to extract information from small-sized systems and use finite-size scaling ideas[3,4] to predict the large system behavior. To this end, at zero temperature, we traditionally have at our disposal properties such as spectral gaps, response functions, and correlation functions; in recent years, entanglement measures, which have been at the heart of proposals for quantum computation,[5,6] have also been used as signatures of quantum critical behavior.[7,8]

While one usually resorts to numerical techniques to calculate these properties for systems ranging from typically tens to hundreds of spins, obtaining them analytically for just a few spins proves extremely useful. Indeed, the corresponding calculations can be particularly simple by exploiting the system's symmetry, and the results can provide data to check the numerical codes devised for larger systems. From the pedagogical point of view, dealing with few spins gives examples of how to add more than two angular momenta in a systematic way. It also sheds light on exploring less familiar probes, such as entanglement.

A particularly interesting example consists of four equally-spaced spins-1/2, fixed in positions on a ring (Fig. 1). We assume that they are coupled through competing exchange interactions J and $J_2 = \alpha J$ between nearest- and next-nearest neighbors, respectively. Quantum effects are brought about by considering scalar interactions involving the three cartesian spin components. The Hamiltonian may therefore be expressed in terms of spin operators, $\mathbf{S}_i$, $i = 1-4$, as

$$\mathcal{H} = J\left[\sum_{i=1}^{4} \mathbf{S}_i \cdot \mathbf{S}_{i+1} + \alpha \sum_{i=1}^{4} \mathbf{S}_i \cdot \mathbf{S}_{i+2}\right], \tag{1}$$

with $\mathbf{S}_5 \equiv \mathbf{S}_1$ and $\mathbf{S}_6 \equiv \mathbf{S}_2$, thus setting up periodic boundary conditions. For reasons that will become apparent, we always consider $J_2 \geq 0$, so that the sign of α is the same as that of J. A semiclassical analysis for $\alpha = 0$ immediately reveals that if $J < 0$, the ground state corresponds to all spins aligned (ferromagnetic state, FM), e.g., $|\uparrow\uparrow\uparrow\uparrow\rangle$, while if $J > 0$ the spins are in an antiferromagnetic (AFM) (or Néel-like) state, e.g., $|\uparrow\downarrow\uparrow\downarrow\rangle$. Therefore, when $\alpha > 0$, a large J_2 disrupts the AFM state, favoring a dimerized state, $|\uparrow\downarrow\downarrow\uparrow\rangle$; by the same token, when $\alpha < 0$, a large J_2 also favors a dimerized state.[*] An interesting issue is to determine the ground state evolution as J_2 increases from zero, for both $\alpha > 0$ and $\alpha < 0$. Here, we will use addition of four angular momenta to obtain simple expressions for both the eigenstates and energies of $\mathcal{H}$, from which we discuss the different "phase transitions" based on level crossings, correlation functions, and entanglement entropy. As discussed later, this example with four spins allows a much more diverse and illustrative analysis of entanglement than with just two spins.

The outline of the paper is as follows. In Sec. II, we present a diagonalization of $\mathcal{H}$ based on the addition of four spins-1/2, and discuss its spectrum. This solution allows us to obtain in Sec. III the spin–spin correlation functions for the different ground states. In Sec. IV, we explore the fact that there are three different ways of splitting a four-spin system into two parts (one and three spins, two pairs of non-adjacent spins, and two pairs of adjacent spins) to compare how their entanglement entropies pinpoint α-driven quantum critical points. Finally, in Sec. V, we briefly discuss the main features of this model as unveiled by calculations on larger systems.

II. ENERGY SPECTRUM

The angular momentum eigenvalue problem for a single spin-s particle is defined by

$$\mathbf{S}_i^2 |s_i m_i\rangle = s_i(s_i+1)\hbar^2 |s_i m_i\rangle, \tag{2}$$

$$S_i^z |s_i m_i\rangle = m_i \hbar |s_i m_i\rangle, \tag{3}$$

[*]The reader should note that when $J_2 < 0$ there is no competition with J, irrespective of the sign of the latter.

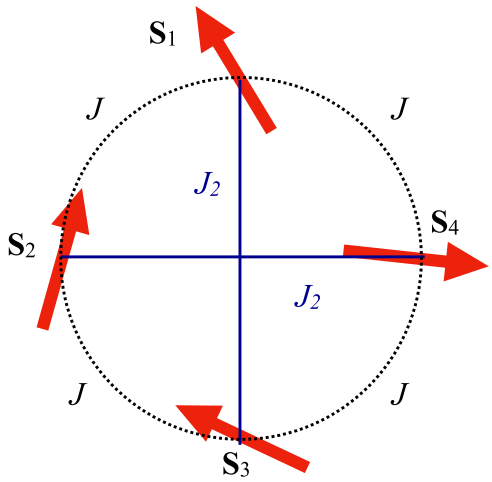

Fig. 1. A semiclassical representation of the four spins on a ring; J and J_2 are the exchange coupling constants between spins on nearest (dotted lines) and next-nearest neighbor sites (solid lines), respectively.

where $\mathbf{S}_i^2 \equiv \mathbf{S}_i \cdot \mathbf{S}_i$, $i = 1-4$, and S_i^z is the z component of $\mathbf{S}_i$; their associated quantum numbers are s_i and $m_i = -s_i, -s_i+1, \ldots, s_i$. For four spin-1/2 particles, the state space is 16-dimensional, and a possible basis may be taken as $\{|s_1 m_1 s_2 m_2 s_3 m_3 s_4 m_4\rangle\}$. Since the labels s_i reflect an intrinsic attribute of the particles, they remain fixed and may be omitted to simplify the notation; that is, we refer to this basis as $\{|m_1 m_2 m_3 m_4\rangle\}$, with $m_i = \pm 1/2$ (or $\uparrow, \downarrow$, for short). In this basis, the Hamiltonian is a block diagonal matrix, each block being characterized by the value of $M = \sum_{i=1}^4 m_i$; this block structure reflects the built-in axial symmetry of the basis due to the conservation of the z component of the total spin, $S_T^z \equiv S_1^z + S_2^z + S_3^z + S_4^z$.

However, the Hamiltonian symmetry is actually higher than this: it is invariant under a simultaneous rotation of *all* spins by any angle around *any* axis. That is, the total angular momentum is conserved, as expected classically in the absence of an external torque. However, quantum-mechanically, the non-commutation of the components of angular momentum operators does not allow their simultaneous determination. At any rate, further simplicity should arise by changing to a higher-symmetry basis, e.g., to one labeled by the total angular momentum quantum number, S_T, in addition to M, which is the quantum number associated with S_T^z.

The total spin operator is

$$\mathbf{S}_T = \mathbf{S}_1 + \mathbf{S}_2 + \mathbf{S}_3 + \mathbf{S}_4, \tag{4}$$

and its square may be written as

$$\mathbf{S}_T^2 = K_0 + 2K_1 + K_2, \tag{5}$$

where we have introduced

$$K_0 \equiv \sum_{i=1}^4 \mathbf{S}_i^2, \tag{6}$$

$$K_1 \equiv \sum_{i=1}^4 \mathbf{S}_i \cdot \mathbf{S}_{i+1}, \tag{7}$$

$$K_2 \equiv \sum_{i=1}^4 \mathbf{S}_i \cdot \mathbf{S}_{i+2}. \tag{8}$$

Thus, the Hamiltonian, Eq. (1), may be expressed as

$$\mathcal{H} = J[K_1 + \alpha K_2], \tag{9}$$

where we note that periodic boundary conditions for four sites imply that the coupling between any two second-neighbor spins appears twice in the Hamiltonian; redefining α solely for four sites would not allow direct comparison of critical points with larger lattices.

Our aim now is to determine a basis in which $\mathcal{H}$ is expressed solely in terms of eigenvalues of the operators $K_0, K_1,$ and K_2. According to the rules for addition of more than two angular momenta, one adds two spins at a time and subsequently adds up the results.[9] We may then evaluate K_2 by taking the square of the partial sums $\mathbf{S}_{13} \equiv \mathbf{S}_1 + \mathbf{S}_3$ and $\mathbf{S}_{24} \equiv \mathbf{S}_2 + \mathbf{S}_4$,

$$\mathbf{S}_{13}^2 = \mathbf{S}_1^2 + \mathbf{S}_3^2 + 2\,\mathbf{S}_1 \cdot \mathbf{S}_3, \tag{10}$$

$$\mathbf{S}_{24}^2 = \mathbf{S}_2^2 + \mathbf{S}_4^2 + 2\,\mathbf{S}_2 \cdot \mathbf{S}_4, \tag{11}$$

and adding them to obtain, with the aid of Eqs. (6) and (8),

$$K_2 = \mathbf{S}_{13}^2 + \mathbf{S}_{24}^2 - K_0. \tag{12}$$

Taking this into Eq. (5) leads to

$$K_1 = \frac{1}{2}\left[\mathbf{S}_T^2 - (\mathbf{S}_{13}^2 + \mathbf{S}_{24}^2)\right]. \tag{13}$$

We note that $\mathbf{S}_T^2$, $\mathbf{S}_i^2$, with $i = 1-4$, and $\mathbf{S}_{ii+2}^2$, with $i = 1, 2$ are scalar operators; as such, they commute with each other as well as with S_T^z. Therefore, $\mathscr{C} \equiv \{\mathbf{S}_T^2, S_T^z, \mathbf{S}_{13}^2, \mathbf{S}_{24}^2, \mathbf{S}_1^2, \mathbf{S}_2^2, \mathbf{S}_3^2, \mathbf{S}_4^2\}$ forms a complete set of commuting observables (CSCOs, see, e.g., Ref. 10).

The Hamiltonian can then be cast in the form

$$\mathcal{H} = \frac{J}{2}\left[\mathbf{S}_T^2 - 2\alpha K_0 + (2\alpha - 1)(\mathbf{S}_{13}^2 + \mathbf{S}_{24}^2)\right], \tag{14}$$

and since (14) is expressed solely in terms of operators in $\mathscr{C}$, we may replace the operators by their respective eigenvalues when using this basis. The eigenvalues can be determined by systematically adding up spins, starting with the partial sums, $\mathbf{S}_{13}$ and $\mathbf{S}_{24}$: the possible quantum numbers for the square of these partial sums are $s_{ii+2} = 0, 1$, for $i = 1, 2$. We then add up $\mathbf{S}_T = \mathbf{S}_{13} + \mathbf{S}_{24}$, which leads to the possible quantum numbers $S_T = 0, 1, 2$, associated with $\mathbf{S}_T^2$. The eigenenergies can finally be expressed in terms of S_T, s, s_{13}, and s_{24}:

$$\frac{E}{|J|\hbar^2} = \mathrm{sign}(\alpha)\frac{1}{2}\{S_T(S_T+1) - 8\alpha s(s+1) + (2\alpha - 1)[s_{13}(s_{13}+1) + s_{24}(s_{24}+1)]\}, \tag{15}$$

Table I. Quantum numbers for the addition of four spins-1/2. The partial sum of two spins-1/2 yields the quantum numbers $s_{13} = 0, 1$ and $s_{24} = 0, 1$; A given pair of values of s_{13} and s_{24} yields the total spin quantum number as $S_T = |s_{13} - s_{24}|, |s_{13} - s_{24}| + 1, \ldots, s_{13} + s_{24}$. Since the total angular momentum is conserved, the energy degeneracy for each total spin multiplet is $g_S = 2S_T + 1$.

s_{13}	0	1	0	1	1	1
s_{24}	0	0	1	1	1	1
S_T	0	1	1	0	1	2
g_S	1	3	3	1	3	5

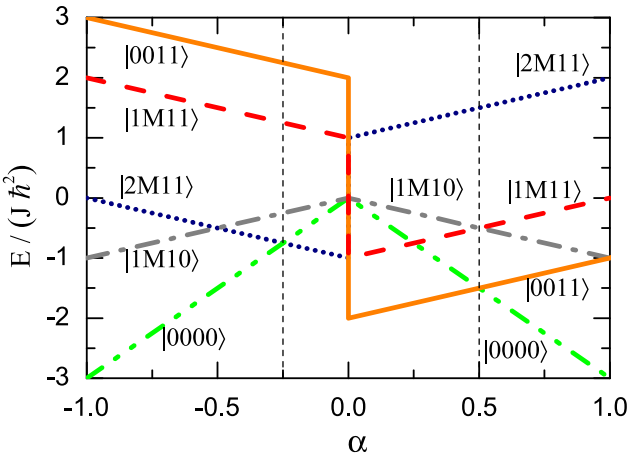

Fig. 2. Energy eigenvalues for the four-site J-J_2 Heisenberg model as a function of $\alpha \equiv J_2/J$, with $J_2 > 0$; the curves are labeled by $|S_T M s_{13} s_{24}\rangle$ and we recall that the states $|1M10\rangle$ and $|1M01\rangle$ are degenerate.

where $\text{sign}(\alpha) \equiv \alpha/|\alpha| = J/|J|$ is the sign function, which is positive if $\alpha > 0$ and negative if $\alpha < 0$. As expected, the energies do not depend on the orientation of the ring since there is no preferred direction in space. The degeneracy in $M = -S_T, -S_T + 1, \ldots S_T$ of each level is $g_S = 2S_T + 1$. Table I lists all possible combinations of the quantum numbers entering in the evaluation of the energies. The eigenvectors may then be denoted by $|S_T M s_{13} s_{24}\rangle$, where, since they have a constant value, we keep omitting $s_1, \ldots, s_4$. The corresponding eigenenergies are plotted as functions of α in Fig. 2.

It will often prove illustrative to express the lowest energy eigenstates in terms of a "split basis," formed by $\{|s_{13} m_{13}\rangle \otimes |s_{24} m_{24}\rangle\}$; see Appendix A. Note that the split basis is composed of two two-spin states, each corresponding to the sublattices {1,3} and {2,4}.

If $-1/4 < \alpha < 0$, the ground state is the ferromagnetic quintuplet,[†] $|2M11\rangle$, $M = -2, -1, 0, 1, 2$; see Eqs. (A3) and (A7)–(A10). By contrast, if $\alpha < -1/4$, the ground state is the singlet

$$|0000\rangle = |00\rangle \otimes |00\rangle, \tag{16}$$

which may be thought of as a superposition of dimerized states. Thus, the nature of the ground state changes at $\alpha_{c,1} = -1/4$, which suggests that this crossing point in the ground state energies evolves into a quantum critical point as the number of sites, L, increases; more on this below.

If $\alpha > 0$, the second-neighbor coupling frustrates the tendency of forming a Néel-like state, $|\uparrow\downarrow\uparrow\downarrow\rangle$. Indeed, Fig. 2 shows that if $0 < \alpha < 1/2$, the ground state is a different singlet,

$$|0011\rangle = \frac{1}{\sqrt{3}}[|1-1\rangle \otimes |11\rangle - |10\rangle \otimes |10\rangle + |11\rangle \otimes |1-1\rangle] \tag{17}$$

[see Eq. (A19)], which is a superposition of pairs (1,3) and (2,4) forming triplets that add up in such a way to yield a global singlet; note that each term in the superposition has $M = m_{13} + m_{24} = 0$.

[†]By "ferromagnetic," we mean all states which have $M \neq 0$.

Beyond $\alpha = \alpha^* = 1/2$, the ground state is the same singlet as for $\alpha < -1/4$; see Eq. (16). As we will see, the correlation functions highlight the difference between these two singlets.

III. SPIN–SPIN CORRELATION FUNCTIONS

The spin–spin correlation function is defined as

$$\mathscr{S}(r) \equiv \langle \mathbf{S}_i \cdot \mathbf{S}_{i+r} \rangle, \tag{18}$$

thus measuring the influence a spin variable at site i exerts on the value of the spin variable at a site separated by a distance r; at zero temperature, the averages $\langle \cdots \rangle$ are understood as ground state expectation values. If $\mathscr{S} > 0$, spins i and $i+r$ are correlated, whereas, for $\mathscr{S} < 0$, they are anticorrelated.

Translational invariance allows us to write

$$\mathscr{S}(r) = \frac{1}{4}\langle K_r \rangle, \quad r = 0, 1, 2. \tag{19}$$

We note that $r = 2$ is the maximum distance in this case due to periodic boundary conditions. In a macroscopic system, the behavior at large distances, $r \gg 1$, probes the existence and the nature of microscopic ordering. Since here we are dealing with only four sites, we cannot make any claims about the long distance behavior of $\mathscr{S}(r)$. Nonetheless, even for four sites, $\mathscr{S}(r)$ provides useful insights into the nature of the different ground states, as we will see below.

Similar to the eigenenergies, the $\langle K_r \rangle$'s may be expressed in terms of the eigenvalues of the operators in $\mathscr{C}$, to yield

$$\mathscr{S}(0) = S_T(S_T+1)\hbar^2, \tag{20}$$

$$\mathscr{S}(1) = \frac{1}{8}[S_T(S_T+1) - s_{13}(s_{13}+1) - s_{24}(s_{24}+1)]\hbar^2, \tag{21}$$

$$\mathscr{S}(2) = \frac{1}{4}[s_{13}(s_{13}+1) + s_{24}(s_{24}-1) - 4S_T(S_T+1)]\hbar^2. \tag{22}$$

The correlation functions for the different ground states (corresponding to the different regimes of α) are displayed in Fig. 3. Note that $\mathscr{S}(0) \equiv \langle \mathbf{S}_i^2 \rangle = (3/4)\hbar^2$ is the same for all ground states. When the ground state is the singlet $|0000\rangle$ [Eq. (16)], spins on the same sublattice are maximally anticorrelated, since

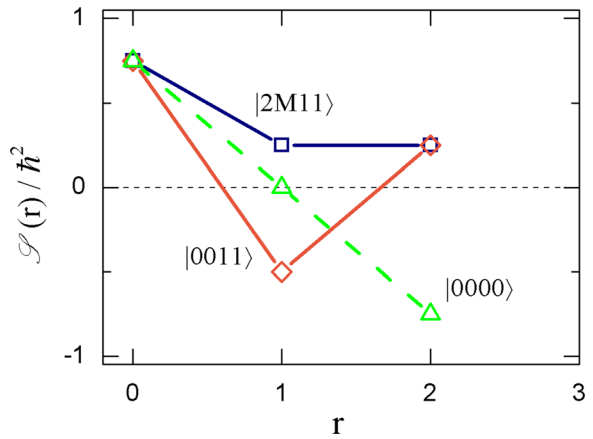

Fig. 3. Correlation functions corresponding to the different ground states, $|S_T M s_{13} s_{24}\rangle$, of a four-site ring, as functions of the distance between spins.

they are in two-spin singlet states; spins on different sublattices, on the other hand, are uncorrelated. This should be contrasted with the behavior for the overall singlet, $|0011\rangle$ [Eq. (17)], which is made up from two-spin triplets. Indeed, members of the two-spin triplets are positively correlated, but they are negatively correlated with a spin in the other sublattice. For $\alpha = 0$ and $J > 0$, the triplets would be antiparallel to each other. Also noteworthy is the overall decay in the magnitude of $\mathscr{S}(r)$, which may be attributed to the fact that a superposition of several states, such as in Eq. (17), enhances fluctuations at long distances.

The correlation function for the quintuplet $|2M11\rangle$ does not depend on M since the basis satisfies rotational invariance. Had we expressed the ground state in terms of $\{|m_1 m_2 m_3 m_4\rangle\}$, the equality $\langle S_i^z S_{i+r}^z\rangle = (1/4)\langle S_i^+ S_{i+r}^- + S_i^- S_{i+r}^+\rangle$ would have only held by averaging each side of this equation over M. This shows the advantage of using a higher-symmetry basis. Figure 3 also shows the correlation function for any member of the quintuplet: all spins are positively correlated, in accordance with the classical picture of a ferromagnetic state. Another feature distinguishable from the singlet cases is that $\mathscr{S}(r)$ is a constant beyond $r = 1$. For a L-site ring, $L > 4$, it is easy to see that this holds for the saturated ferromagnetic state, $|M| = L\hbar/2$. The constant correlation function illustrates a fundamental difference between the FM state and those generically referred to as AFM states as can be appreciated by examining the $\alpha = 0$ case. The FM Hamiltonian, $J < 0$, can be mapped onto the AFM Hamiltonian by a transformation U that takes $\mathbf{S}_i \to -\mathbf{S}_i$ in one sublattice, say the set of odd-labeled sites. Thus, each of the FM ground states, $|F\rangle$, satisfying $\mathcal{H}_F|F\rangle = E_F|F\rangle$, is taken onto a state $|\Phi\rangle = U^\dagger|F\rangle$, which satisfies $\mathcal{H}_A|\Phi\rangle = -\mathcal{H}_F|\Phi\rangle = E_F|\Phi\rangle$. Note that the state $|\Phi\rangle$ is not the ground state of the AFM Hamiltonian, since the spectrum is not symmetric. Instead, with the AFM ground state being a superposition of states with $M = 0$, the correlations alternate in sign and magnitude, as shown in Fig. 3; the AFM ground state is therefore characterized by intense quantum fluctuations.

IV. ENTANGLEMENT

A. Two spins

To introduce the concept of entanglement, let us first consider the case of two spins-1/2. The possible states, $|S_T M\rangle$, are a singlet state $|00\rangle$ and the triplet states $|11\rangle$, $|1-1\rangle$, and $|10\rangle$. The states with $M \neq 0$ are *separable*, that is, $|11\rangle = |\uparrow\rangle \otimes |\uparrow\rangle$ and $|1-1\rangle = |\downarrow\rangle \otimes |\downarrow\rangle$. On the other hand, the $M = 0$ states cannot be written as a direct product of single-particle states since $|10\rangle = (1/\sqrt{2})[|\uparrow\rangle \otimes |\downarrow\rangle + |\downarrow\rangle \otimes |\uparrow\rangle]$ and $|00\rangle = (1/\sqrt{2})[|\uparrow\rangle \otimes |\downarrow\rangle - |\downarrow\rangle \otimes |\uparrow\rangle]$. In the latter cases, we say that the spins are entangled: in a bipartite entangled spin state, the determination of the state of one spin necessarily implies knowledge of the other spin.[11]

One way to identify whether or not two parts of a system are entangled is through the density operator, ρ. If one can ascertain that a system is definitely in an arbitrary state $|\psi\rangle$, one says that the system is in a pure state, and the density operator, defined by $\rho \equiv |\psi\rangle\langle\psi|$, is such that $\rho^2 \equiv \rho$. By contrast, if one has limited amount of information about a system, in the sense that it has a probability p_1 of being in the state $|\psi_1\rangle$, a probability p_2 of being in the state $|\psi_2\rangle$, and so forth, with $\sum_k p_k = 1$, one says that the system is in a statistical mixture of states or *mixed state*. A familiar example is provided by a system in the canonical ensemble, in which case $p_k = (1/Z)\exp(-E_k/k_B T)$, where $|\psi_k\rangle$ is the eigenstate of the Hamiltonian associated with the eigenvalue E_k, k_B is the Boltzmann constant, T is the absolute temperature, and Z is the partition function. Note also that a statistical mixture should not be confused with a superposition of pure states, $|\psi\rangle = \sum_k c_k|\psi_k\rangle$, which displays interference effects between different $|\psi_k\rangle$'s; these effects, in turn, are absent in the mixture. In other words, one cannot associate a quantum state with a mixture. Nonetheless, we can still define a density operator for a mixture as the weighted average of the density operators, that is,

$$\rho \equiv \sum_k p_k \rho_k, \quad \text{with} \quad \rho_k \equiv |\psi_k\rangle\langle\psi_k|. \tag{23}$$

Therefore, if the $|\psi_k\rangle$'s are orthonormalized, one has

$$\rho^2 = \sum_k p_k^2 \rho_k \leq \sum_k p_k \rho_k = \rho. \tag{24}$$

Since the equality only holds for a pure system, $\rho^2 \neq \rho$ may be taken as a signature of a mixed state.

Returning to the case of two spins, we note that the four states, $|S_T M\rangle$, are all pure states, those with $M = 0$ being written as superpositions of $|\uparrow\downarrow\rangle$ and $|\downarrow\uparrow\rangle$. For these entangled states, if we focus on, say, the first spin, it is not in a definite state since it is equally probable to be found either up or down; hence, although the two-spin state is a pure state, the first spin is in a mixed state. By contrast, for the separable ($M = \pm 1$) states, the first spin is in a definite state [being up (down) in the $M = 1$ ($M = -1$) state]; hence, the first spin is in a pure state. The conclusion is that spins 1 and 2 are entangled if each one is in a mixed state, and, conversely, they are separable if each one is in a pure state. Therefore, a qualitative measure of the entanglement between spins 1 and 2 may be given by the reduced density operator for one of the spins obtained by taking the partial trace of the density operator ρ on the sub-space corresponding to the second spin. For instance, considering $\rho = |10\rangle\langle 10|$, we trace out the second spin,

$$\tilde{\rho}(1) \equiv \mathrm{Tr}_2\, \rho, \tag{25}$$

where the operation Tr_2 is the trace restricted to the Hilbert space corresponding to the second particle, by calculating the matrix elements,[12]

$$\langle m_1|\tilde{\rho}(1)|m_1'\rangle = \sum_{m_2=\uparrow,\downarrow} \langle m_1 m_2|10\rangle\langle 10|m_1' m_2\rangle. \tag{26}$$

We have $\tilde{\rho}(1) = 1/2 \cdot \mathbb{1}_2$, where $\mathbb{1}_d$ is the $d \times d$ identity matrix. Since $[\tilde{\rho}(1)]^2 \neq \tilde{\rho}(1)$, spin 1 is not in a pure state: it is therefore entangled with spin 2.

One may also use a quantitative measure of entanglement, namely the von Neumann entropy associated with the reduced density operator,[11]

$$S(1) = -\sum_{i=1}^{2} \lambda_i \ln \lambda_i, \tag{27}$$

where λ_1 and λ_2 are the two eigenvalues of $\tilde{\rho}(1)$; in the present case, $\lambda_1 = \lambda_2 = 1/2$, so that $S(1) = \ln 2$, which is the maximum possible entanglement for two spins-1/2.[11] By

contrast, the entropy is zero for separable states such as $|\uparrow\uparrow\rangle$ and $|\downarrow\downarrow\rangle$.

B. Four spins

Extending these ideas to the present case of four spins, we note that there are three nonequivalent ways of partitioning the system into two subsystems: spins 1 and 3 could be grouped together, or spins 1 and 2, or spins 2, 3 and 4; we denote these partitions by (13)–(24), (12)–(34), and (1)–(234), respectively. Note that the first partition involves the good quantum numbers s_{13} and s_{24}, so one expects features different from the (12)–(34) partition. We now consider each of these bipartite cases in turn.

1. Subsystems (13) and (24)

The state $|0000\rangle = |00\rangle_{13} \otimes |00\rangle_{24}$ can be written as a direct product of two pairs of singlets, (13) and (24). This is also manifest by taking the partial trace[12] over spins 2 and 4 to obtain the reduced density operator,

$$\begin{aligned}\tilde{\rho}(13) &= \mathrm{Tr}_{s_{24},m_{24}}|00\rangle_{13} \otimes |00\rangle_{24\ 13}\langle 00|\otimes_{24}\langle 00| \\ &= |00\rangle_{13\ 13}\langle 00|\ \mathrm{Tr}_{s_{24},m_{24}}|00\rangle_{24\ 24}\langle 00| \\ &= |00\rangle_{13\ 13}\langle 00|, \end{aligned} \tag{28}$$

since $\mathrm{Tr}_{s_{24},m_{24}}|00\rangle_{24\ 24}\langle 00| = 1$. Thus,

$$[\tilde{\rho}(13)]^2 = \tilde{\rho}(13), \tag{29}$$

so that the (13) subsystem is in a pure state, hence separable from (24). This is hardly surprising, given that the ground state is a direct product of pure states. Accordingly, the eigenvalues of $\tilde{\rho}(13)$ are 1 and 0 (threefold degenerate), which leads to a vanishing von Neumann entropy.

We now discuss the ground state for $0 < \alpha < 1/2$, namely, $|0011\rangle$, as given by Eq. (A19). Unlike $|0000\rangle$ [Eq. (A23)], one sees by inspection that spins 1 and 3 are entangled with spins 2 and 4: the state $|0011\rangle$ is a superposition of states, such that if one determines $|s_{13}m_{13}\rangle$, the state $|s_{24}m_{24}\rangle$ is readily determined. Furthermore, following steps similar to those in Eq. (28), we obtain the reduced density operator,

$$\tilde{\rho}(13) = \frac{1}{3}[|1-1\rangle\langle 1-1| + |10\rangle\langle 10| + |11\rangle\langle 11|], \tag{30}$$

which, in the $|s_{13}m_{13}\rangle$ basis, is represented by

$$\tilde{\rho}(13) = \frac{1}{3}\begin{pmatrix} 1 & 0 & 0 & 0 \\ 0 & 1 & 0 & 0 \\ 0 & 0 & 1 & 0 \\ 0 & 0 & 0 & 0 \end{pmatrix}, \tag{31}$$

and is such that $[\tilde{\rho}(13)]^2 \neq \tilde{\rho}(13)$, so that the partitions (13) and (24) are entangled. With the eigenvalues of $\tilde{\rho}(13)$ being $\lambda = 0$ and $\lambda = 1/3$ (threefold degenerate), the von Neumann entropy becomes

$$S(13) = -\sum_{i=1}^{4} \lambda_i \ln \lambda_i = \ln 3, \tag{32}$$

yet another signature of entanglement.

In the interval $-1/4 < \alpha < 0$, the ground state is the quintuplet $S_T = 2$, with two separable states, $|2 \pm 211\rangle = |1 \pm 1\rangle_{13} \otimes |1 \pm 1\rangle_{24}$, and three entangled states, $|2 \pm 111\rangle$ and $|2011\rangle$; see Eqs. (A7)–(A9). The reduced density matrices (now with a subscript corresponding to the value of m_{13}) are

$$\tilde{\rho}_1(13) = \frac{1}{2}\begin{pmatrix} 1 & 0 & 0 & 0 \\ 0 & 1 & 0 & 0 \\ 0 & 0 & 0 & 0 \\ 0 & 0 & 0 & 0 \end{pmatrix}, \quad \tilde{\rho}_{-1}(13) = \frac{1}{2}\begin{pmatrix} 0 & 0 & 0 & 0 \\ 0 & 0 & 0 & 0 \\ 0 & 0 & 1 & 0 \\ 0 & 0 & 0 & 1 \end{pmatrix}, \tag{33}$$

and

$$\tilde{\rho}_0(13) = \frac{1}{6}\begin{pmatrix} 1 & 0 & 0 & 0 \\ 0 & 4 & 0 & 0 \\ 0 & 0 & 1 & 0 \\ 0 & 0 & 0 & 0 \end{pmatrix}. \tag{34}$$

The von Neumann entropies for the five states are

$$S_{\pm 2}(13) = 0, \tag{35}$$

$$S_{\pm 1}(13) = \ln 2, \tag{36}$$

$$S_0(13) = \ln 3 - \frac{1}{3}\ln 2, \tag{37}$$

so that among this quintuplet, the maximally entangled state is the one with $M = 0$, corresponding to the largest number of possibilities for m_{13} (and consequently for m_{24}) in the linear combination, Eq. (A8).

2. Subsystems (12) and (34)

Let us then investigate what happens when we consider as subsystems the pairs (12) and (34). In this case, however, we must express the density operators in the basis of individual spins (see Appendix B) and trace out spins 3 and 4. The matrix elements of the reduced density operator, $\tilde{\rho}_{12}$, are

$$\langle m_1 m_2|\tilde{\rho}_{12}|m_1' m_2'\rangle = \sum_{m_3 m_4} \langle m_1 m_2 m_3 m_4|\rho|m_1' m_2' m_3 m_4\rangle. \tag{38}$$

For $\rho = |0000\rangle\langle 0000|$, we take Eq. (B16) into Eq. (38) to obtain

$$\tilde{\rho}_{12} = \frac{1}{4}\mathbb{1}_4. \tag{39}$$

Since $\tilde{\rho}_{12}^2 \neq \tilde{\rho}_{12}$, the subsystem (12) is not pure, meaning that (12) and (34) are entangled. The eigenvalues of $\tilde{\rho}_{12}$ are $\lambda = 1/4$ (fourfold degenerate), so that the von Neumann entropy is $S(12) = 2\ln 2$.

In the interval $0 < \alpha < 1/2$, the density operator is $\rho = |0011\rangle\langle 0011|$ [see Eq. (B9)], and the trace over m_3 and m_4 yields

$$\tilde{\rho}(12) = \frac{1}{12}\begin{pmatrix} 1 & 0 & 0 & 0 \\ 0 & 5 & -4 & 0 \\ 0 & -4 & 5 & 0 \\ 0 & 0 & 0 & 1 \end{pmatrix}, \tag{40}$$

whose eigenvalues are $\lambda = 1/12$ (threefold degenerate) and 3/4, so that the von Neumann entropy is

$$S(12) = 2\ln 2 - \frac{1}{2}\ln 3. \tag{41}$$

And, finally, for $-1/4 < \alpha < 0$, the same structure found for $\tilde{\rho}_{m_{13}}$ applies: the $M = \pm 2$ states are separable, while the states with $M = 0, \pm 1$ are entangled. Again with the aid of the basis of individual spins, Eq. (38) yields the reduced density operators as

$$\tilde{\rho}_1(12) = \frac{1}{4}\begin{pmatrix} 2 & 0 & 0 & 0 \\ 0 & 1 & 1 & 0 \\ 0 & 1 & 1 & 0 \\ 0 & 0 & 0 & 0 \end{pmatrix}, \quad \tilde{\rho}_{-1}(12) = \frac{1}{4}\begin{pmatrix} 0 & 0 & 0 & 0 \\ 0 & 1 & 1 & 0 \\ 0 & 1 & 1 & 0 \\ 0 & 0 & 0 & 2 \end{pmatrix}, \tag{42}$$

and

$$\tilde{\rho}_0(12) = \frac{1}{6}\begin{pmatrix} 1 & 0 & 0 & 0 \\ 0 & 2 & 2 & 0 \\ 0 & 2 & 2 & 0 \\ 0 & 0 & 0 & 1 \end{pmatrix}. \tag{43}$$

The associated von Neumann entropies are then

$$S_{\pm 2}(12) = 0, \tag{44}$$

$$S_{\pm 1}(12) = \ln 2, \tag{45}$$

$$S_0(12) = \ln 3 - \frac{1}{3}\ln 2, \tag{46}$$

which are identical to the ones obtained for the partition (13)–(24). This indicates that the entanglement properties of the ground states in this quintuplet are not sensitive to the way the system is partitioned in half.

3. Subsystems (1) and (234)

Consider now the partition into, say, spin 1 on the one hand and spins 2, 3, and 4 on the other. The elements of the single-spin reduced matrix, $\tilde{\rho}_1$, are then given by

$$\langle m_1|\tilde{\rho}_1|m_1'\rangle = \sum_{m_2 m_3 m_4} \langle m_1 m_2 m_3 m_4|\rho|m_1' m_2 m_3 m_4\rangle. \tag{47}$$

For the state $|0000\rangle$, we have

$$\tilde{\rho}(1) = \frac{1}{4}\mathbb{1}_2. \tag{48}$$

Since $[\tilde{\rho(1)}]^2 \neq \tilde{\rho}(1)$, spin 1 is entangled with the remaining spins, and the entropy is $S(1) = \ln 2$.

Similarly, for the state $|0011\rangle$, Eq. (47) yields

$$\tilde{\rho}(1) = \frac{1}{2}\mathbb{1}_2, \tag{49}$$

which leads to the same entropy as for the state $|0000\rangle$.

For the quintuplet of states, we start with $|2 \pm 211\rangle$,

$$\tilde{\rho}_2(1) = \begin{pmatrix} 1 & 0 \\ 0 & 0 \end{pmatrix} \quad \text{and} \quad \tilde{\rho}_{-2}(1) = \begin{pmatrix} 0 & 0 \\ 0 & 1 \end{pmatrix}, \tag{50}$$

both of which lead to $S_{\pm 2}(1) = 0$, as it should for a separable state. For the states $|2 \pm 111\rangle$, we take Eqs. (B2) and (B4) into Eq. (47) to obtain, respectively,

$$\tilde{\rho}_1(1) = \frac{1}{4}\begin{pmatrix} 3 & 0 \\ 0 & 1 \end{pmatrix} \quad \text{and} \quad \tilde{\rho}_{-1}(1) = \frac{1}{4}\begin{pmatrix} 1 & 0 \\ 0 & 3 \end{pmatrix}, \tag{51}$$

whose entropies are $S_{\pm 1}(1) = 2\ln 2 - (3/4)\ln 3$. Finally, the reduced density matrix for $|2011\rangle$ becomes $\tilde{\rho}_0(1) = (1/2)\mathbb{1}_2$, and the associated entropy is $S_0(1) = \ln 2$.

C. Overall discussion of the entropies

The discussion of Sec. IV B illustrates that when we split a spin system, the parts bear the signature of how entangled the subsystems are with each other. This in turn reflects the multiplicity of states accessible to the individual spins within the remaining part, which is captured by the entropy. Indeed, Fig. 4 shows the entropy as a function of α for each choice of partition. In the FM region, $-1/4 < \alpha < 0$, there are always three different values of the entropy depending on the value of $|M|$. As $|M|$ increases, the number of states of the superposition decreases, leading to a decreasing entropy until a minimum value of zero for the saturated states $|M| = 2$. When the system is partitioned according to the partial sums, $\mathbf{S}_{13}$

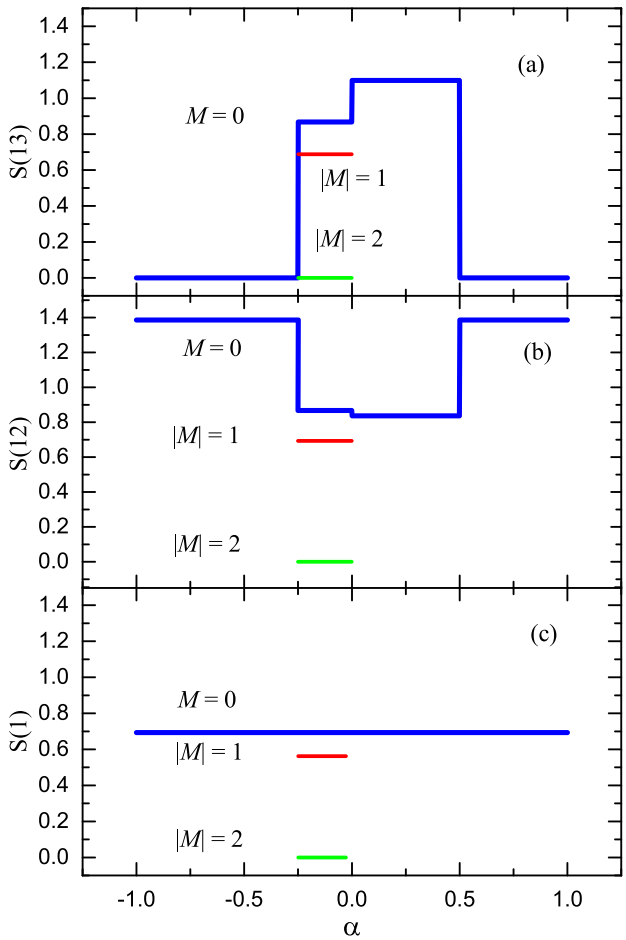

Fig. 4. Ground state entanglement entropies as functions of α: (a) $S(13)$, which measures entanglement between spins on different sublattices, (b) $S(12)$, which measures entanglement between dimers, and (c) $S(1)$, which measures entanglement between a single spin and the remaining ones. In all panels, the entropy depends on $|M|$ in the region $-1/4 < \alpha < 0$.

and $\mathbf{S}_{24}$, one has separable states for all α, except in the range $0 < \alpha < 1/2$. By contrast, by choosing the (12)–(34) partition, the system is maximally entangled when the ground state is $|0000\rangle$, as given by Eq. (16): this was to be expected, since spins 1 and 3, as well as 2 and 4, form singlets and are therefore entangled. Finally, when the partition involves one spin and three spins, the entanglement is uniform. These findings indicate that coupling q-bits in a controlled way gives rise to a wider range of entanglements that can be exploited in quantum computation.[5]

V. COMMENTS ON LARGER SYSTEMS

For completeness, we note that numerical studies of this model have been carried out for much larger lattice sizes, L,[13–15] which allowed to extrapolate the spectral data for $L \to \infty$. Figure 5 compares the phase diagrams for the four-site ring with the one obtained through different numerical methods in the thermodynamic limit.[13–16] We see that the FM phase is already present for $L = 4$, and its boundaries are the same as in the thermodynamic limit. By contrast, when $L = 4$ the ground state for $\alpha < -1/4$ is $|0000\rangle$, while in the thermodynamic limit it is an incommensurate state, which means that the spatial period of the magnetic arrangement is not an integer multiple of the lattice spacing; one may think of classical vectors whose tips describe a spiral as one moves along the lattice without actually returning to the initial orientation at a lattice site. This difference is due to the fact that the $L = 4$ system is too small to accommodate an incommensurate spin arrangement. For $\alpha > 0$, the thermodynamic limit predicts a second-order phase transition between a spin liquid (SL) and a dimerized (D) state taking place at $\alpha_c \approx 0.2411$. The SL phase may be thought of as a superposition of singlets, involving pairs of spins on all possible sites; this results in gapless excitations and power-law decay of the spin–spin correlation function. The D phase may be thought of as superposition of singlets, involving pairs of spins on nearby sites only; this results in gapped excitations and exponential decay of the spin–spin correlation function. Here also, the ground states for $L = 4$ do not resemble their $L \to \infty$ counterparts: The state $|0011\rangle$ is a superposition of direct products of triplet states, and the state $|0000\rangle$ is a direct product of next-nearest-neighbor singlets. Again, the smallness of the $L = 4$ ring accounts for these differences, which should decrease as L increases. Indeed, the transitions involving these subtle phases can only be identified on systems of size $L \gtrsim \xi$, where ξ is the correlation length; however, by examining data for *different sizes*, one may extrapolate to the thermodynamic limit using finite-size scaling theories.[3,4,17]

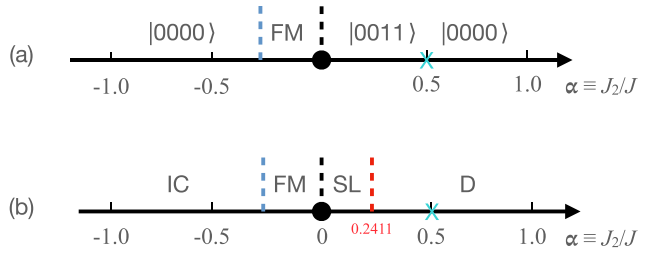

Fig. 5. (a) The phase diagram for the four-site ring, where the kets follow the notation of Fig. 2, and FM corresponds to the quintuplets $|2M11\rangle$. (b) The phase diagram obtained from different numerical approaches allowing for extrapolations to the thermodynamic limit (Refs. 13–16). IC stands for incommensurate spiral phase, FM for saturated ferromagnetic phase, SL for spin liquid, and D for dimerized.

Another interesting feature is that $\alpha = \alpha_{MG} \equiv 1/2$ marks the point (the so-called Majumdar–Ghosh point[16]) at which the dimerized ground state is doubly degenerate: Nearest-neighbor dimers form between sites 1 and 2, 3 and 4, 5 and 6, and so forth, or between sites 2 and 3, 4 and 5, 6 and 7, and so forth. For the $L = 4$ ring, we found that the singlet-from-singlets state and the singlet-from-triplets state cross exactly at α_{MG}, which indeed suggests that, for larger systems, similar crossings should occur at this point.

VI. CONCLUSIONS

By considering a small number of interacting spins, we have illustrated how to add more than two angular momenta, and, for an evenly spaced four spin-1/2 ring, how the addition algorithm provides a set of actual eigenstates of the Hamiltonian. We have analyzed entanglement and illustrated how the different ways of splitting the system in two parts leads to different quantitative measures of entanglement. We believe that the problem treated here should attract the interest of students and educators involved in quantum mechanics courses: (1) addition of four spins goes beyond the usual examples of addition of just two angular momenta, while tractable; (2) this addition problem is applied to determine the spectrum of an interacting system; (3) the solution thus obtained is used to illustrate how correlation functions are important to characterize some physical properties of a spin system; and (4) it is also applied to introduce entanglement and characterize it through different quantities.

It is useful to present a few suggestions for natural follow-ups: First, we recall that some of the eigenstates for $L = 4$ (see Fig. 5) do not display the same features as the corresponding ones in the thermodynamic limit. It would therefore be illustrative to perform calculations for $L = 6, 8, \ldots$, and examine the symmetries of the various ground states. This would demand implementing symmetries, such as the translational symmetry setting up basis states, and performing computer (numerical or algebraic) diagonalizations. Analyses of correlations and entanglement (also as a quantum critical point marker) would also add considerable insight.

A second line to pursue is that of spin ladders: instead of a single chain with L sites, one can consider two spin chains (initially with nearest-neighbor couplings along the chain direction, i.e., $\alpha = 0$) coupled through exchange interactions, J', between spins on the same rung.[18] One could consider ladders with $L = 6, 8, \ldots$ sites along the chain direction and investigate how the ground state evolves with J/J' either by numerical diagonalizations or through perturbation theory. Again, correlation functions and entanglement properties could be studied once the ground state is determined.

We can also make some comments related to multipartite entanglement (ME). Many definitions and measures of ME have been proposed throughout the years (see, e.g., Ref. 8), and it is still a very active area of research. A simple example, applicable to the present context of quantum phase transitions in spin systems, is that of global entanglement (GE), defined as[19]

$$E_G^{(1)} = 2 - \frac{2}{L}\sum_{j=1}^{L} \mathrm{Tr}\,\rho_j^2, \tag{52}$$

where $\rho_j = \mathrm{Tr}_k \rho$ is the reduced single-spin density matrix, obtained by taking the partial trace of the full density operator, ρ, over all spins at sites $k \neq j$. A generalized version of this entanglement measure[20] is

$$E_G^{(2)} = \frac{1}{L-1} \sum_{\ell=1}^{L-1} G(2,\ell), \tag{53}$$

where $0 < \ell < L$ is the distance between two spins, and

$$G(2,\ell) = \frac{4}{3}\left(1 - \frac{1}{L-\ell}\sum_{j=1}^{L-\ell} \mathrm{Tr}\,\rho_{j,j+\ell}^2\right), \tag{54}$$

with $\rho_{j,j+\ell}$ being the reduced density matrix for spins j and $j+\ell$, obtained from the partial trace over the other $L-2$ spins. In the thermodynamic limit, both measures reach a maximum value at the quantum critical point of the transverse Ising model;[20] it is therefore legitimate to wonder whether these quantities are equally useful in locating the critical points of the frustrated Heisenberg model discussed here, when $L \to \infty$.

Finally, it is worth mentioning that competing interactions along the lines considered here have been invoked to explain the magnetic behavior of materials such as $CuGe0_3$,[21,22] $SrCuO_2$,[23] and, more recently, a szenicsite.[24]

ACKNOWLEDGMENTS

The authors are grateful to the Brazilian Agencies CAPES, CNPq, National Institute for Science and Technology on Quantum Information, and FAPERJ for financial support.

AUTHOR DECLARATIONS

Conflict of Interest

The authors have no conflicts of interest.

APPENDIX A: THE SPLIT BASIS

Here, we discuss how to express the states $|S_T M s_{13} s_{24}\rangle$ as linear combinations of direct products $|s_{13} m_{13}\rangle \otimes |s_{24} m_{24}\rangle$; we refer to these as *the split basis*. Since

$$\langle S_T M s'_{13} s'_{24} | [|s_{13} m_{13}\rangle \otimes |s_{24} m_{24}\rangle] = 0, \quad \text{if } s'_{13} \neq s_{13} \text{ or } s'_{24} \neq s_{24}, \tag{A1}$$

for a fixed pair (s_{13}, s_{24}), we may write

$$|S_T M s_{13} s_{24}\rangle = \sum_{m_{13}+m_{24}=M} a_{m_{13},m_{24}} |s_{13} m_{13}\rangle \otimes |s_{24} m_{24}\rangle, \tag{A2}$$

so that the Hilbert space is decomposed into subspaces $\mathcal{E}_{s_{13},s_{24}}$ with dimensions $(2s_{13}+1)\cdot(2s_{24}+1)$. The coefficients $a_{m_{13},m_{24}}$ are known as the Clebsch–Gordan coefficients (see, e.g., Ref. 25), which we will determine explicitly, for completeness.

We start with the state with the largest S_T, namely $S_T = 2$, and $M = S_T = 2$ (Table I). The only possible correspondence for this state is

$$|2211\rangle = |11\rangle \otimes |11\rangle, \tag{A3}$$

where from now on we adopt the convention that the first (second) ket on the RHS is relative to the pair (1,3) ((2,4)).

Recalling that each one of the ladder operators,

$$S_T^{\pm} \equiv S_{13}^{\pm} + S_{24}^{\pm}, \tag{A4}$$

changes the value of M by one unit, that is (see, e.g., Ref. 26),

$$S_T^{\pm} |S_T M\rangle = \hbar \sqrt{S_T(S_T+1) - M(M\pm 1)}\, |S_T\, M \pm 1\rangle, \tag{A5}$$

we apply S_T^- to both sides of Eq. (A3) to obtain

$$\begin{aligned} S_T^- |2211\rangle &= 2\hbar |2111\rangle \\ &= [S_{13}^- + S_{24}^-]\,[|11\rangle \otimes |11\rangle] \\ &= \sqrt{2}\hbar [|10\rangle \otimes |11\rangle + |11\rangle \otimes |10\rangle], \end{aligned} \tag{A6}$$

from which we extract

$$|2111\rangle = \frac{1}{\sqrt{2}}[|10\rangle \otimes |11\rangle + |11\rangle \otimes |10\rangle]. \tag{A7}$$

Now we further decrease M by one unit, still considering the $S_T = 2$ states. Following the same steps leading to Eq. (A7), we arrive at

$$|2011\rangle = \frac{1}{\sqrt{6}}[|1-1\rangle \otimes |11\rangle + 2|10\rangle \otimes |10\rangle + |11\rangle \otimes |1-1\rangle]. \tag{A8}$$

The states $|2-111\rangle$ and $|2-211\rangle$ are obtained by flipping all spins in Eqs. (A7) and (A3), respectively,

$$|2-111\rangle = \frac{1}{\sqrt{2}}[|10\rangle \otimes |1-1\rangle + |1-1\rangle \otimes |10\rangle] \tag{A9}$$

and

$$|2-211\rangle = |1-1\rangle \otimes |1-1\rangle. \tag{A10}$$

Our next task is to express the states with $S_T = 1$ in the split basis. Similar to Eq. (A7), we may write

$$|1111\rangle = a|10\rangle \otimes |11\rangle + b|11\rangle \otimes |10\rangle, \tag{A11}$$

where the coefficients a and b are chosen by both orthogonalizing the state with respect to Eq. (A7),

$$\langle 2111|1111\rangle = \frac{1}{\sqrt{2}}(a+b) = 0 \quad \Rightarrow \quad b = -a, \tag{A12}$$

and normalization. We end up with

$$|1111\rangle = \frac{1}{\sqrt{2}}[|10\rangle \otimes |11\rangle - |11\rangle \otimes |10\rangle]. \tag{A13}$$

Starting from Eq. (A13), we repeat the procedure above to generate the states corresponding to $M < 1$; we obtain

$$|1011\rangle = \frac{1}{\sqrt{2}}[|1-1\rangle \otimes |11\rangle - |11\rangle \otimes |1-1\rangle], \tag{A14}$$

$$|1-111\rangle = \frac{1}{\sqrt{2}}[|10\rangle \otimes |1-1\rangle - |1-1\rangle \otimes |10\rangle]. \tag{A15}$$

We finally arrive at the last state arising from $S_{13} = S_{24} = 1$, namely, $|0011\rangle$. It may be obtained by writing

$$|0011\rangle = a|11\rangle \otimes |1-1\rangle + b|10\rangle \otimes |10\rangle + c|1-1\rangle \otimes |11\rangle, \tag{A16}$$

with the coefficients being determined by orthogonalization,

$$\langle 2011|0011\rangle = \frac{1}{\sqrt{6}}[c + 2b + a] = 0, \tag{A17}$$

$$\langle 1011|0011\rangle = \frac{1}{\sqrt{6}}[c - a] = 0, \tag{A18}$$

together with normalization; thus,

$$|0011\rangle = \frac{1}{\sqrt{3}}[|1-1\rangle \otimes |11\rangle - |10\rangle \otimes |10\rangle + |11\rangle \otimes |1-1\rangle]. \tag{A19}$$

Now we consider the cases with $S_{13} = 1$ and $S_{24} = 0$, which leads solely to $S_T = 1$. We may thus identify

$$|1110\rangle = |11\rangle \otimes |00\rangle, \tag{A20}$$

to which we successively apply Eq. (A4) to obtain

$$|1010\rangle = |10\rangle \otimes |00\rangle, \tag{A21}$$

$$|1-110\rangle = |1-1\rangle \otimes |00\rangle. \tag{A22}$$

The three states obtained by considering $S_{13} = 0$ and $S_{24} = 1$ are obtained by interchanging the kets on the RHS of Eqs. (A20)–(A22).

Finally, the total singlet made up by the combination of two partial singlets is

$$|0000\rangle = |00\rangle \otimes |00\rangle, \tag{A23}$$

thus completing the 16 states of the split basis.

It is worth noting that some of the states in the split basis are separable, or disentangled (i.e., written in terms of a single direct product), while others are not separable, or entangled.

APPENDIX B: THE INDIVIDUAL BASIS

We may also write the eigenstates in terms of individual spin states, $\{|m_1 m_2 m_3 m_4\rangle\}$. Indeed, since $|11\rangle = |\uparrow\uparrow\rangle$ Eq. (A3) yields

$$|2211\rangle = |\uparrow\uparrow\uparrow\uparrow\rangle. \tag{B1}$$

Similarly, with $|10\rangle = \left(1/\sqrt{2}\right)[|\uparrow\downarrow\rangle + |\downarrow\uparrow\rangle]$, Eq. (A7) yields

$$|2111\rangle = \frac{1}{2}[|\downarrow\uparrow\uparrow\uparrow\rangle + |\uparrow\downarrow\uparrow\uparrow\rangle + |\uparrow\uparrow\downarrow\uparrow\rangle + |\uparrow\uparrow\uparrow\downarrow\rangle], \tag{B2}$$

and

$$|2011\rangle = \frac{1}{\sqrt{6}}[|\uparrow\uparrow\downarrow\downarrow\rangle + |\uparrow\downarrow\downarrow\uparrow\rangle + |\downarrow\downarrow\uparrow\uparrow\rangle + |\downarrow\uparrow\uparrow\downarrow\rangle + (|\uparrow\downarrow\uparrow\downarrow\rangle + |\downarrow\uparrow\downarrow\uparrow\rangle)], \tag{B3}$$

with the remaining states with $S_T = 2$ being given by flipping all spins in $|2111\rangle$ and $|2-211\rangle$, that is,

$$|2-111\rangle = \frac{1}{2}[|\uparrow\downarrow\downarrow\downarrow\rangle + |\downarrow\uparrow\downarrow\downarrow\rangle + |\downarrow\downarrow\uparrow\downarrow\rangle + |\downarrow\downarrow\downarrow\uparrow\rangle] \tag{B4}$$

and

$$|2-211\rangle = |\downarrow\downarrow\downarrow\downarrow\rangle. \tag{B5}$$

Still with $s_{13} = s_{24} = 1$, we have the eigenstates with $S_T = 1$, namely,

$$|1111\rangle = \frac{1}{2}[|\uparrow\uparrow\downarrow\uparrow\rangle + |\downarrow\uparrow\uparrow\uparrow\rangle - |\uparrow\uparrow\uparrow\downarrow\rangle - |\uparrow\downarrow\uparrow\uparrow\rangle], \tag{B6}$$

$$|1011\rangle = \frac{1}{\sqrt{2}}[|\downarrow\uparrow\downarrow\uparrow\rangle - |\uparrow\downarrow\uparrow\downarrow\rangle], \tag{B7}$$

$$|1-111\rangle = \frac{1}{2}[|\downarrow\downarrow\uparrow\downarrow\rangle + |\uparrow\downarrow\downarrow\downarrow\rangle - |\downarrow\downarrow\downarrow\uparrow\rangle - |\downarrow\uparrow\downarrow\downarrow\rangle], \tag{B8}$$

as well as the one with $S_T = 0$,

$$|0011\rangle = \frac{1}{\sqrt{3}}\left[|\uparrow\downarrow\uparrow\downarrow\rangle + |\downarrow\uparrow\downarrow\uparrow\rangle - \frac{1}{2}(|\uparrow\uparrow\downarrow\downarrow\rangle + |\uparrow\downarrow\downarrow\uparrow\rangle + |\downarrow\uparrow\uparrow\downarrow\rangle + |\downarrow\downarrow\uparrow\uparrow\rangle)\right]. \tag{B9}$$

For $s_{13} = 1$ and $s_{24} = 0$, Eqs. (A20)–(A22) yield

$$|1110\rangle = \frac{1}{\sqrt{2}}[|\uparrow\uparrow\uparrow\downarrow\rangle - |\uparrow\downarrow\uparrow\uparrow\rangle], \tag{B10}$$

$$|1010\rangle = \frac{1}{2}[|\uparrow\uparrow\downarrow\downarrow\rangle - |\uparrow\downarrow\downarrow\uparrow\rangle + |\downarrow\uparrow\uparrow\downarrow\rangle - |\downarrow\downarrow\uparrow\uparrow\rangle], \tag{B11}$$

$$|1-110\rangle = \frac{1}{\sqrt{2}}[|\downarrow\downarrow\downarrow\uparrow\rangle - |\downarrow\uparrow\downarrow\downarrow\rangle], \tag{B12}$$

while for $s_{13} = 0$ and $s_{24} = 1$, we have

$$|1101\rangle = \frac{1}{\sqrt{2}}[|\uparrow\uparrow\downarrow\uparrow\rangle - |\downarrow\uparrow\uparrow\uparrow\rangle], \tag{B13}$$

$$|1001\rangle = \frac{1}{2}[|\uparrow\uparrow\downarrow\downarrow\rangle + |\uparrow\downarrow\downarrow\uparrow\rangle - |\downarrow\uparrow\uparrow\downarrow\rangle - |\downarrow\downarrow\uparrow\uparrow\rangle], \tag{B14}$$

$$|1-101\rangle = \frac{1}{\sqrt{2}}[|\downarrow\downarrow\uparrow\downarrow\rangle - |\uparrow\downarrow\downarrow\downarrow\rangle]. \tag{B15}$$

And, finally, Eq. (A23) leads to

$$|0000\rangle = \frac{1}{2}[|\downarrow\downarrow\uparrow\uparrow\rangle - |\uparrow\downarrow\downarrow\uparrow\rangle + |\uparrow\uparrow\downarrow\downarrow\rangle - |\downarrow\uparrow\uparrow\downarrow\rangle]. \tag{B16}$$

[a]ORCID: 0000-0002-4469-621X.
[b]Present address: Departamento de Física, PUC/Rio, Rio de Janeiro, Brazil, ORCID: 0000-0002-3965-0268.
[c]ORCID: 0000-0003-4285-4672

[1]S. Sachdev, *Quantum Phase Transitions*, 2nd ed. (Cambridge U.P., Cambridge, MA, 2011).
[2]M. Continentino, *Quantum Scaling in Many-Body Systems: An Approach to Quantum Phase Transitions*, 2nd ed. (Cambridge U.P., Cambridge, MA, 2017).
[3]M. E. Fisher, "Critical phenomena," in *Proceedings of the Enrico Fermi International School of Physics*, edited by M. S. Green (Academic Press, New York, 1971), Vol. 51.
[4]M. N. Barber, "Finite-size scaling," in *Phase Transitions and Critical Phenomena*, edited by C. Domb and J. L. Lebowitz (Academic Press, New York, 1983), Vol. 8, p. 145.

[5]M. A. Nielsen and I. L. Chuang, *Quantum Computation and Quantum Information: 10th Anniversary Edition* (Cambridge U.P., Cambridge, MA, 2010).
[6]E. Chitambar and G. Gour, "Quantum resource theories," Rev. Mod. Phys. **91**(2), 025001 (2019).
[7]A. Osterloh, L. Amico, G. Falci, and R. Fazio, "Scaling of entanglement close to a quantum phase transition," Nature **416**(6881), 608–610 (2002).
[8]L. Amico, R. Fazio, A. Osterloh, and V. Vedral, "Entanglement in many-body systems," Rev. Mod. Phys. **80**(2), 517–576 (2008).
[9]A. Messiah, *Quantum Mechanics* (North-Holland, Amsterdam, The Netherlands, 1970), Vol. 2, pp. 566–569.
[10]C. Cohen-Tannoudji, B. Diu, and F. Laloë, *Quantum Mechanics*, 1st ed. (Wiley, New York, NY, 1977), pp. 139–144.
[11]K. Gottfried and T. Yan, *Quantum Mechanics: Fundamentals*, Graduate Texts in Contemporary Physics (Springer, New York, 2003), pp. 39–52.
[12]C. Cohen-Tannoudji, B. Diu, and F. Laloë, *Quantum Mechanics*, 1st ed. (Wiley, New York, NY, 1977), pp. 295–307.
[13]T. Tonegawa and I. Harada, "One-dimensional isotropic spin-1/2 Heisenberg magnet with ferromagnetic nearest-neighbor and antiferromagnetic next-nearest-neighbor interactions," J. Phys. Soc. Jpn. **58**(8), 2902–2915 (1989).
[14]K. Okamoto and K. Nomura, "Fluid-dimer critical point in S = 1/2 antiferromagnetic Heisenberg chain with next nearest neighbor interactions," Phys. Lett. A **169**(6), 433–437 (1992).
[15]R. Zinke, S.-L. Drechsler, and J. Richter, "Influence of interchain coupling on spiral ground-state correlations in frustrated spin-$\frac{1}{2}$ J_1–J_2 Heisenberg chains," Phys. Rev. B **79**(9), 094425 (2009).
[16]C. K. Majumdar and D. K. Ghosh, "On next-nearest neighbor interaction in linear chain. II," J. Math. Phys. **10**(8), 1399–1402 (1969).
[17]R. R. dos Santos and R. B. Stinchcombe, "Finite size scaling and crossover phenomena: The XY chain in a transverse field at zero temperature," J. Phys. A **14**(10), 2741–2757 (1981).
[18]E. Dagotto and T. M. Rice, "Surprises on the way from one- to two-dimensional quantum magnets: The ladder materials," Science **271**(5249), 618–623 (1996).
[19]D. A. Meyer and N. R. Wallach, "Global entanglement in multiparticle systems," J. Math. Phys. **43**(9), 4273–4278 (2002).
[20]T. R. de Oliveira, G. Rigolin, and M. C. de Oliveira, "Genuine multipartite entanglement in quantum phase transitions," Phys. Rev. A **73**(1), 010305 (2006).
[21]M. Hase, I. Terasaki, and K. Uchinokura, "Observation of the spin-Peierls transition in linear Cu^{2+} (spin-1/2) chains in an inorganic compound $CuGeO_3$," Phys. Rev. Lett **70**(23), 3651–3654 (1993).
[22]G. Castilla, S. Chakravarty, and V. J. Emery, "Quantum magnetism of $CuGeO_3$," Phys. Rev. Lett. **75**(9), 1823–1826 (1995).
[23]M. Matsuda and K. Katsumata, "Magnetic properties of a quasi-one-dimensional magnet with competing interactions: $SrCuO_2$," J. Magn. Magn. Mater. **140–144**, 1671–1672 (1995).
[24]A. Berlie and I. Terry, "Possible realization of the Majumdar-Ghosh point in the mineral Szenicsite," Phys. Rev. B **105**(22), L220404 (2022).
[25]A. Messiah, *Quantum Mechanics* (North-Holland, Amsterdam, The Netherlands, 1970), Vol. 2, pp. 560–563.
[26]A. Messiah, *Quantum Mechanics* (North-Holland, Amsterdam, The Netherlands, 1970), Vol. 2, pp. 510–516.

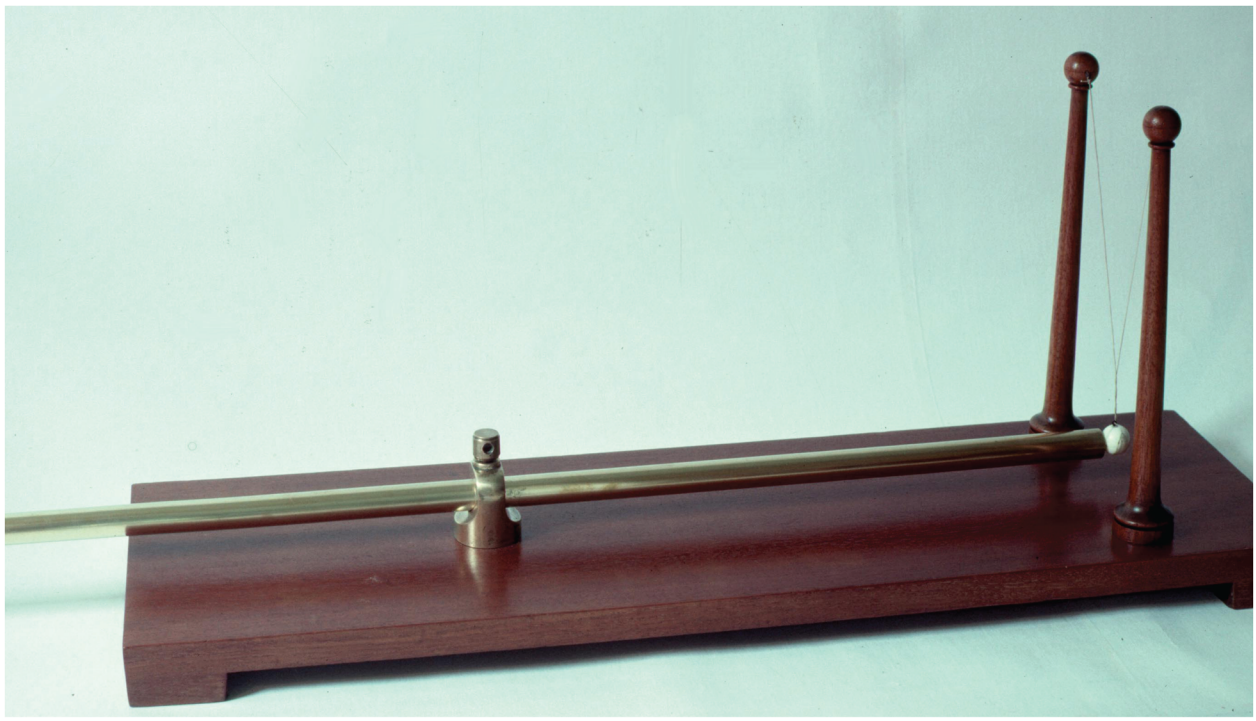

The Ringing Bar

I used this piece of apparatus for demonstrations for nearly forty years at Kenyon College, and never used it in its intended form! As made, the ivory ball rested gently against the end of the brass rod. When the free end of the rod was stroked with a rosined cloth, longitudinal vibrations were set up, and the ball sprang to the side. I noticed the clear pitch when the ball stuck the end of the rod and used it to find the speed of sound in brass. The frequency of the sound was determined beating it against the sound produced by a speaker driven by a function generator. The length of the rod was a half wavelength (ignoring end corrections) and the speed obtained from $v = f\lambda$. (Picture and text by Thomas B. Greenslade, Jr., Kenyon College)